2021_OptMat_Mega_Novita_CIE_Ruby.pdf

by

Submission date: 04-Aug-2022 08:47PM (UTC+0700)
Submission ID: 1878776060
File name: 2021_OptMat_Mega_Novita_CIE_Ruby.pdf (2.05M)
Word count: 4411
Character count: 23590

Optical Materials 121 (2021) 111539

Contents lists available at ScienceDirect

Optical Materials

journal homepage: www.elsevier.com/locate/optmat

Research Article

Chromaticity coordinates of ruby based on first-principles calculation

Mega Novita[a,*], Irna Farikhah[a], Rizky Muliani Dwi Ujianti[a], Dian Marlina[b], Benjamin Walker[c,1], Hironori Kiyooka[d], Shota Takemura[d], Kazuyoshi Ogasawara[d]

[a] Faculty of Engineering and Informatics, Universitas PGRI Semarang, Jl. Sidodadi Timur No. 24 Semarang, Central Java, 50125, Indonesia
[b] Faculty of Pharmacy, Universitas Setia Budi, Jl. Letjend Sutoyo Mojosongo, Surakarta, Central Java, 57127, Indonesia
[c] Dalney Street NW, Atlanta, GA 30318, USA
[d] School of Science and Technology, Kwansei Gakuin University, 2-1 Gakuen Sanda, Hyogo, 669-1337, Japan

ARTICLE INFO

Keywords:
Ruby
First-principles
Chromaticity
Color
Coordinate

ABSTRACT

Understanding the local atomic configuration is crucial for studying phosphor materials. Their performance in many applications is strongly dependent upon their optical properties. Much experimental and theoretical effort has been made to meet the requirements. Specifically, *ab-initio* studies have extensively reported the absorption spectra and the multiplet energies of phosphors. However, the qualitative analysis of the emitted light has not yet been reported. In this work, we characterized the emitted light of ruby, which is a widely studied phosphor material. The absorption spectra of ruby were calculated utilizing the non-empirical discrete variational Xα (DV-Xα) and discrete variational multi-electron (DVME) software. Then, the investigation on the (x,y) chromaticity coordinates of was performed under the standard illuminant D65 utilizing ColorAC software, a chromaticity diagram maker. In this work, we used a ruby model cluster generated from an α-Al_2O_3 crystal. The model consists of seven atoms, where one chromium atom surrounded by six oxygen atoms. We compared the absorption spectra obtained via simple configuration interaction (CI) and those obtained which include energy corrections called configuration dependent correction (CDC) and correlation correction (CC). We successfully reproduced the color that is observed in experiment. The chromaticity coordinates approach red region for higher concentration. The results show that the calculation with CDC-CC shows better agreement with experiment. This research confirms the non-empirical calculations based on the DV-Xα and DVME methods, in the terms of emitted light.

1. Introduction

In the study of phosphor materials, it is very important to understand the local atomic arrangement. The quantum mechanical calculations, also known as first-principles calculations, have therefore gained increased importance not only for deep understanding of various basic properties of materials, but also for design and development of many kinds of new phosphor materials. For several decades, the density functional theory (DFT) calculation method has been employed to solve various problems in material science [1,2]. Various DFT methods have been shown to be very useful for the calculation of molecular orbital and band structure calculations including discrete variational Xα (DV-Xα) method [3–5], plane wave basis pseudopotential (PWPP) [6,7], full potential linearized augmented plane wave (FLAPW) method [8], and Orthogonalized Linear Combination of Atomic Orbitals (OLCAO) method [9–11].

The transitions between multiplets of the impurity states of phosphor materials play an important role in the luminescent process. Basically, these multiplets are determined by the local structure of the material. In order to correctly assign the multiplets from the experiment, accurate information on electronic state and chemical bonding is needed. Unfortunately, there are some difficulties which cannot be solved by the above theoretical approaches. Ordinary DFT calculations based on one-electron methods could not directly calculate the multiplets; therefore, first-principles many-electron calculations i.e. configuration interaction (CI) method should be employed to solve this type of problem. To calculate multiplet states of transition-metal ions in crystals, Ogasawara et al. [12–16] created discrete variational multi-electron (DVME) software, which is based on DV-Xα molecular orbital (MO) method. This method has been used effectively on a series of crystals doped with either rare earth or transition metal ions [17–27]. Although multiplets can be directly calculated in simple CI calculations, those energies are

* Corresponding author.
E-mail address: novita@upgris.ac.id (M. Novita).
[1] Independent Researcher.

https://doi.org/10.1016/j.optmat.2021.111539
Received 7 August 2021; Received in revised form 26 August 2021; Accepted 29 August 2021

generally overestimated. On the other hand, although the average energy of multiplets can be well reproduced in a DFT calculation, the multiplets cannot be directly calculated. To decrease the overestimation, CI calculations with corrections based on one-electron DFT calculations were introduced. Even if the theoretical and the observed spectra are more closely aligned when CI is coupled with corrections, the qualitative color reproduced by the theoretical phosphor material is not clear.

In the eye, there are three different types of cones: S, M, and L. The S-cones are responsible for short-wavelength sensitivity, the M-cones for middle-wavelength sensitivity, and the L-cones for long-wavelength sensitivity. This means that the human eye is only capable of detecting red, green, and blue and the brain then extrapolates all other colors based on the intensities of the original three colors. In the 1920s, William David Wright and the International Commission on Illumination (CIE) set out to measure the wavelength sensitivity of each of these cones developing the CIE standard observer color matching functions and the color space chromaticity diagram [28,29]. With this information, it became possible to qualitatively measure the color of an object as perceived by a standard observer for the first time. This event is regarded as the beginning of colorimetry.

According to the science of colors, chromaticity is one of the common color parameters used for characterization the emitted light. It can be calculated from the absorption spectrum. The most widely-used model comes from the Commission Internationale d'Eclairage (CIE 1931) [30–32]. As the name implies, the chromaticity diagram is an array of potential colors. Each color is specified by a pair of a numerical coordinates, called the chromaticity coordinate. We may use the chromaticity diagram to show how different hues of light mix together. The pure spectral hues of the rainbow are represented by the points on the curved border. Note that any color inside the diagram can be made in different ways, and only colors around the edge of the diagram are unique colors.

For about a decade, we have been studied the optical properties of ruby, such as lattice relaxation effect, molecular orbitals, multiplet energies, absorption spectra, and pressure dependence, [19–21]. Although non-empirical studies have been conducted, qualitative analysis of the emitted light has not been reported. Therefore, in this work, we characterized the emitted light of ruby. The absorption spectra of ruby were calculated with the non-empirical DV-Xα and DVME software. Then, the (x, y) chromaticity coordinates were investigated using ColorAC software. This research is important in confirming the non-empirical characterization of emitted light based on the DV-Xα and DVME methods.

2. Computational procedure

As illustrated in Fig. 1, seven-atom model clusters were built on a host α-Al_2O_3 crystal with Rh_2O_3 structure [33]. To generate the effective Madelung potential, a Cr^{3+} ion was placed in the cluster's core and approximately 13,600-point charges were placed at the outer atomic sites of the cluster. The local structure of the cluster (C_3 symmetry) was preserved during the calculation; 20,000 sample points were used.

Because the DVME technique is discussed in its entirety in Ref. [14], only the mathematical formulation required to understand the results in this study is explained. We first calculated the molecular orbital using the one-electron DV-Xα method, followed by the optical spectra calculations using the many-electron CI calculations as the main core of the DVME method.

In the one-electron calculations, only one electron is considered. The interaction with the other electrons are averaged and treated just as a potential. The Schrödinger equation for the one-electron calculation is expressed as

$$h\psi(\boldsymbol{r}) = \varepsilon\psi(\boldsymbol{r}) \tag{1}$$

The one-electron Hamiltonian is expressed as

$$h(\boldsymbol{r}) = -\frac{1}{2}\nabla^2 + V(\boldsymbol{r}) \tag{2}$$

The effective molecular potential $V(\boldsymbol{r})$ is expressed as

$$V(\boldsymbol{r}) = -\sum_v \frac{Z_v}{|\boldsymbol{r} - \boldsymbol{R}_v|} + \int \frac{\rho(\boldsymbol{r}')}{|\boldsymbol{r}' - \boldsymbol{r}|} d\boldsymbol{r}' + V_{xc}\{\rho(\boldsymbol{r})\} - 3\alpha\left\{\frac{3}{8\pi}\rho(\boldsymbol{r})\right\}^{1/3} \tag{3}$$

where α is 0.7 and the electron density $\rho(\boldsymbol{r})$ is given by

$$\rho(\boldsymbol{r}) = \sum_l \rho_l(\boldsymbol{r}) = \sum_l f_l |\varphi_l(\boldsymbol{r})|^2 \tag{4}$$

where f_l is the occupancy.

The Schrödinger equation for many-electron calculation is expressed

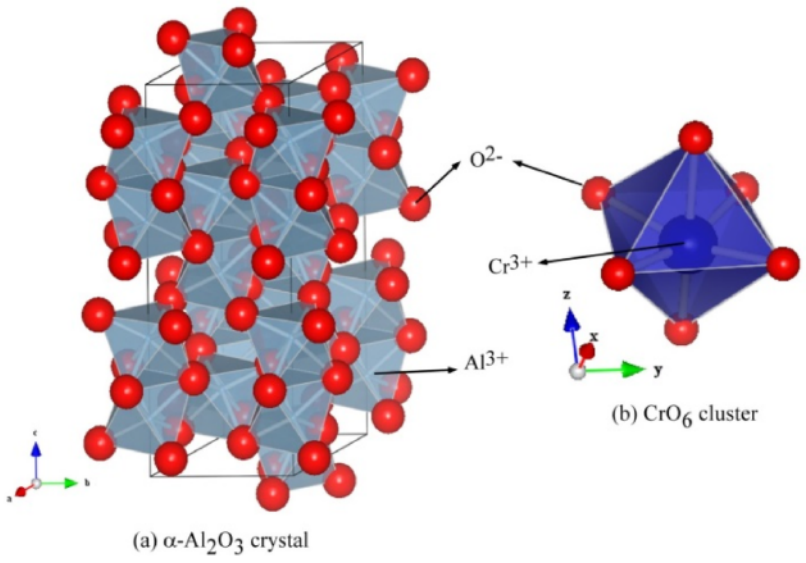

Fig. 1. (a) α-Al_2O_3 crystal structure obtained from Sawada et al. [33] and (b) CrO_6 model cluster used in the calculations.

as

$$H\Psi_I = E\Psi_I \tag{5}$$

Here, electron-electron interactions are directly calculated. The many-electron wave function is expressed as

$$\Psi_I = \sum_{j=1}^{N} W_{jI}\Phi_j \tag{6}$$

W_{jI} is the coefficient of the Slater determinants (Φ_j) used in this calculation, which is expressed as

$$\Phi_j(\mathbf{r}_1, \ldots, \mathbf{r}_n) = \frac{1}{\sqrt{n!}}\begin{vmatrix} \varphi_{j1}(\mathbf{r}_1) & \varphi_{j1}(\mathbf{r}_2) & \cdots & \varphi_{j1}(\mathbf{r}_n) \\ \varphi_{j2}(\mathbf{r}_1) & \varphi_{j2}(\mathbf{r}_2) & \cdots & \varphi_{j2}(\mathbf{r}_n) \\ \vdots & \vdots & \ddots & \vdots \\ \varphi_{jn}(\mathbf{r}_1) & \varphi_{jn}(\mathbf{r}_2) & \cdots & \varphi_{jn}(\mathbf{r}_n) \end{vmatrix} \tag{7}$$

Here, r denotes the electron's location. φ_j's are the molecular orbitals that mostly consist of M 3d orbitals generated from DV-Xα MO calculations. The effective many-electron Hamiltonian for explicitly treated N electrons is written as

$$H = \sum_{i=1}^{N} h(\mathbf{r}_i) + \sum_{i=1}^{N}\sum_{j>i}^{N}\frac{1}{r_{ij}}, \tag{8}$$

where r_{ij} denotes the distance between the ith electron and the jth electron, and h denotes the one-electron operators, which may be written as

$$h(\mathbf{r}_i) = -\frac{1}{2}\nabla_i^2 + V_{nuc}(\mathbf{r}_i) + V_0(\mathbf{r}_i). \tag{9}$$

V_{nuc} denotes the potential owing to the nuclei, whereas V_0 denotes the potential due to the other electrons. As a results, only electrons occupying impurity levels are specifically handled in this calculation. The effective many-electron Hamiltonian can be expanded as follows:

$$\Phi_p|H|\Phi_q = \sum_{i=1}^{N}\sum_{j=1}^{N} A_{ij}^{pq} i|h|j + \sum_{i=1}^{N}\sum_{j=1}^{N}\sum_{k=1}^{N}\sum_{l=1}^{N} B_{ijkl}^{pq} ij|g|kl. \tag{10}$$

H is then diagonalized inside the subspace spanned by the Slater determinants Φ derived from the impurity-state orbitals obtained from the one-electron MO calculations. This step was performed to get the many-electron wave functions and multiplet energies. The many-electron wave functions for each multiplet state may be explicitly calculated as a linear combination of the Slater determinants using the eigenvector obtained by the diagonalized many-electron Hamiltonian. As a result, we can simply calculate the oscillator strength for the electric-dipole transition (transition probability) between multiplets by

$$I_{if} = 2\left(E_f - E_i\right)\left|\Psi_i\left|\sum_{k=1}^{N} \mathbf{r}_k.\mathbf{e}\right|\Psi_f\right|^2 \tag{11}$$

Here, the initial and final states of the many-electron wave functions are denoted by Ψ_i and Ψ_f. Whereas the energy eigenvalues of these states are denoted by E_i and E_f. The unit vector parallel to the direction of the incoming light's electric field is represented by e.

Multiplet energies obtained from many-electron CI calculations are usually underestimated because of the 10–50% overestimation of crystal field splitting [34]. In order to enhance the accuracy of theoretical multiplet energies, numerous adjustments such as configuration dependency correction (CDC) and correlation correction (CC) are considered. In the CDC approach, the barycenters of $(t_{2g})^3$, $(t_{2g})^2(e_g)^1$, $(t_{2g})^1(e_g)^2$, and $(e_g)^3$ configurations were adjusted to be 0, $10Dq$, $20Dq$, and $30Dq$, respectively. Here, the crystal field splitting $10Dq$ was determined using the spin-restricted one-electron MO calculation. On the other hand, in the CC approach, the factor c was calculated from first-principle calculations based on the consistency of the transition energy of the spin-flip transition from $(t_{2g}\uparrow)^3$ to $(t_{2g}\uparrow)^2(t_{2g}\downarrow)^1$ between the many electron CI calculations and the spin-unrestricted one-electron MO calculations. The Hamiltonian with CDC correction is written as

$$\Phi_p\left|H^{CDC}\right|\Phi_q = \sum_{i=1}^{N}\sum_{j=1}^{N} A_{ij}^{pq} i|h|j + \sum_{i=1}^{L}\sum_{j=1}^{L}\sum_{k=1}^{L}\sum_{l=1}^{L} B_{ijkl}^{pq} ij|g|kl + D_{CDC}(m,n)\delta_{pq} \tag{12}$$

where (m,n) denotes the value for $(t_{2g})^m(e_g)^n$ configuration. On the other hand, the Hamiltonian with CC correction is written as

$$\Phi_p\left|H^{CC}\right|\Phi_q = \sum_{i=1}^{N}\sum_{j=1}^{N} A_{ij}^{pq} i|h|j + \sum_{i=1}^{N}\sum_{j=1}^{N}\sum_{k=1}^{N}\sum_{l=1}^{N} c \times B_{ijkl}^{pq} ij|g|kl \tag{13}$$

In this case, the effective Hamiltonian including the CDC and CC effects, is written as

$$\Phi_p\left|H^{CDC-CC}\right|\Phi_q = \sum_{i=1}^{N}\sum_{j=1}^{N} A_{ij}^{pq} i|h|j + \sum_{i=1}^{N}\sum_{j=1}^{N}\sum_{k=1}^{N}\sum_{l=1}^{N} c \times B_{ijkl}^{pq} ij|g|kl + D_{CDC-CC}(m,n)\delta_{pq} \tag{14}$$

In order to analyze the color parameters, the CIE 1931 chromaticity diagram in the ColorAC software is used. The emitted light's color is represented by x and y graph coordinates. This graph is expressed as a red, green, and blue color ratio. These three colors are the X, Y, Z tristimulus values; they correspond to the band-pass filtered chromaticity response of cones in the human retina. The chromaticity coordinates were calculated based on the transmittance which is obtained from absorbance. Transmittance can be defined by

$$T(\lambda) = \frac{I(\lambda)}{I_0(\lambda)} \tag{15}$$

where I_0 is the intensity of incident light while I is that of transmitted light. On the other hand, absorbance can be defined by

$$A(\lambda) = -\log\left(\frac{I(\lambda)}{I_0(\lambda)}\right) \tag{16}$$

Therefore, the transmittance can be calculated by

$$T(\lambda) = e^{-A(\lambda)} \tag{17}$$

Then X, Y, Z can be expressed as

$$\begin{aligned} X &= \int_{380}^{780} T(\lambda)P(\lambda)\bar{x}(\lambda)d\lambda = \int_{380}^{780} e^{-A(\lambda)}P(\lambda)\bar{x}(\lambda)d\lambda \\ Y &= \int_{380}^{780} T(\lambda)P(\lambda)\bar{y}(\lambda)d\lambda = \int_{380}^{780} e^{-A(\lambda)}P(\lambda)\bar{y}(\lambda)d\lambda \\ Z &= \int_{380}^{780} T(\lambda)P(\lambda)\bar{z}(\lambda)d\lambda = \int_{380}^{780} e^{-A(\lambda)}P(\lambda)\bar{z}(\lambda)d\lambda \end{aligned} \tag{18}$$

Here $P(\lambda)$ denotes the standard illuminant D65, which represents natural daylight. Generally, the absorbance is proportional to the molar absorption coefficient ε, the molar concentration of the particles (in this case, chromium ions) c, and the sample thickness l.

$$A(\lambda) = \varepsilon(\lambda)cl \tag{19}$$

Therefore a multiplication of the absorbance by a scalar such as $A_2 = aA_1(\lambda)$ means that the concentration and/or the sample thickness are changed so that $c_2l_2 = ac_1l_1$ is satisfied. Finally, the (x, y) chromaticity coordinates may be derived by

$$x = \frac{X}{X+Y+Z}$$
$$y = \frac{Y}{X+Y+Z} \quad (20)$$

3. Results and discussion

The experimental d-d absorption spectra of ruby published by Fairbank et al. [35] are shown in Fig. 2 together with two theoretical spectra derived from CI calculations without and with CDC-CC correction. The π spectra are represented by solid lines, whereas the σ spectra are represented by dashed lines. The three broad peaks in the measured spectra are assigned as the transition energies from the $^4A_2$ ground state to $^4T_2$, $^4T_{1a}$, and $^4T_{1b}$ states, respectively. It is well-known that these transition energies are generally noted as U-, Y- and Y′- bands, respectively. If we compare the spectra of U-band energy, the σ spectrum is higher than the π spectrum. The situation is opposite for Y- and Y′-band energies. The peak positions of U-, Y-, and Y′-bands are at ~2.2, ~3.0, and ~4.8 eV, respectively. Nevertheless, the peak position in each peak differs slightly between the σ spectrum and the π spectrum.

The three broad peaks and absolute intensities were successfully reproduced in the theoretical spectra. The U-, Y-, and Y′-bands of uncorrected calculations were found at ~2.5, ~3.7 and ~5.7 eV. When the CDC-CC correction was applied, those peaks moved to lower energies at ~2.3, ~3.3 and ~5.0 eV, respectively. The estimated peak positions were enhanced using CDC-CC correction.

Previously, several calculations on ruby have been performed. In 2000, Prof. Ogasawara's group [14] calculated ruby model clusters consisting of 41, 63 and 111 atoms. The TM ion was positioned in the middle of each cluster. In those clusters, 7, 14, and 26 Al ions were included. The effect of structural relaxation was considered by adopting

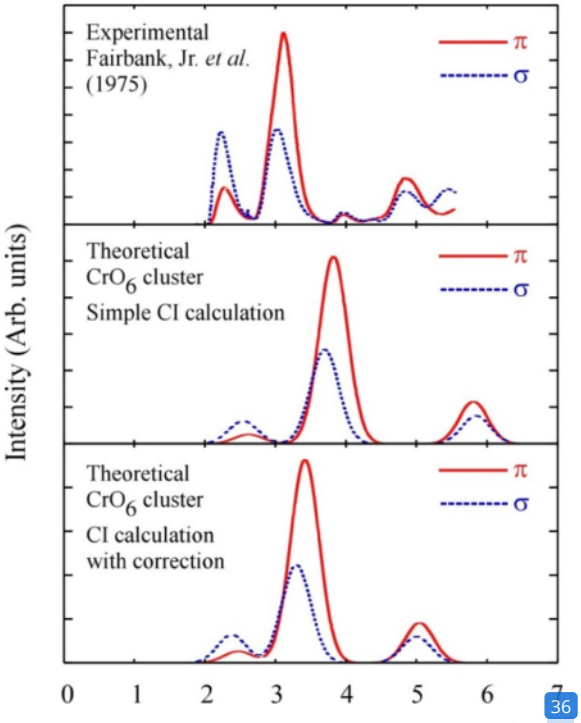

Fig. 2. Experimental and theoretical spectra of ruby (α-Al_2O_3: Cr^{3+}). The experimental spectra were obtained from Fairbank et al. [35] whereas the theoretical spectra were obtained from CI calculations without and with CDC-CC correction using CrO_6 cluster.

the results of Kizler's extended X-ray absorption fine structure (EXAFS) [36]. They also considered the CDC-CC correction to improve the accuracy. We have also performed calculations with a ruby model cluster consisting of 63 atoms [19]. Although we treated the cluster similar to Ref. 9, several computation conditions such as the external atomic sites used to produce Madelung potentials and the sample points were different.

Table 1 shows the comparison of U-, Y- and Y′- bands peak position. As we can see, all of the computational results (except for the results from the simple CI calculation) show good agreement with the experimental data provided by Fairbank et al. [35]. The variation between the current and previous results is very small. However, simple CI calculations overestimated the U-, Y-, and Y′-bands' peak position. These findings imply that simple CI calculations with CDC-CC correction is a good method for accurately predicting the absorption spectra of ruby.

Therefore, based on the absorption spectra obtained in Fig. 2, we then evaluate the (x,y) chromaticity coordinates. It was performed under the standard illuminant D65 obtained from the experimental spectra and the theoretical spectra of CrO_6 cluster that are shown in Fig. 3. The chromaticity coordinates obtained from the experimental spectra are shown by a circle (●); the chromaticity coordinates obtained from theoretical spectra are shown by a triangle (▼); and a square (■) is used to denote CI calculations without and with considering CDC-CC correction. Since the color depends on conditions such as Cr^{3+} concentration and sample thickness and/or density, several points corresponding to different conditions were calculated and plotted. The "experimental color" approaches red for higher concentration. In our calculations, the "theoretical color" obtained without and with considering CDC-CC correction reproduced the same tendency. However, in the case of the CI calculation with CDC-CC corrections, the agreement between the theoretical color and the experimental color is quite good. It indicates that a CI calculation with CDC-CC correction effectively reproduces the absorption spectra of transition metal ions in crystals.

4. Conclusion

The theoretical absorption spectra of ruby were used to compute its chromaticity coordinates under the standard illumination D65. We began by calculating theoretical absorbance spectra with the first-principles DVME technique. The detailed comparison indicates that when CDC-CC correction is considered, the accuracy of the theoretical spectra are considerably enhanced. The numbers of peak, relative intensity between π and σ spectra, as well as the peak positions were well-reproduced in our calculation. These were then displayed on the CIE 1931 color space to get chromaticity coordinates. Next, the result was compared to the experimental data. The higher the concentration, the closer the chromaticity coordinates are to red. The estimated chromaticity coordinates for the spectra obtained by the CI calculation with CDC-CC corrections correspond well with the observed values. Therefore, on the basis of chromaticity coordinates, the agreement between the theoretical spectrum and the experimental spectrum has been quantitatively assessed.

Table 1
The peak position of U-, Y- and Y′- bands of observed spectra and the theoretical spectra.

	U-band (eV)		Y-band (eV)		Y′-band (eV)	
	π	σ	π	σ	π	σ
Expt [35]	2.24	2.27	3.03	3.11	4.85	4.82
Ogasawara [14]	2.31	2.46	3.24	3.40	4.95	4.94
Novita [19]	2.20	2.12	3.17	3.00	4.61	4.60
Simple CI	2.56	2.52	3.80	3.65	5.73	5.81
CI with correction	2.39	2.34	3.42	3.29	5.02	5.05

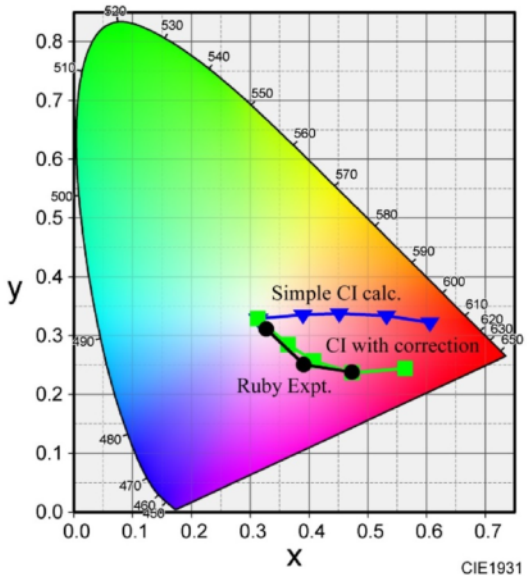

Fig. 3. Chromaticity diagram of experimental and theoretical color coordinates of ruby (α-Al_2O_3: Cr^{3+}). Ruby's experimental data derived from Fairbank's spectra (●) [35]; theoretical absorption spectra obtained from CI calculations without (▾) and with (■) CDC-CC correction using CrO_6 cluster are compared. Various concentrations of Cr^{3+} are represented by points placed along the lines.

Credit authorship contribution statement

Mega Novita: Conceptualization, Methodology, Writing – original draft, Writing – review & editing, Draft. **Irna Farikha:** Investigation, Resources. **Rizky Muliani Dwi Ujianti:** Project administration. **Dian Marlina:** Writing – original draft, Visualization. **Benjamin Walker:** Writing – review & editing, Draft, Proofread. **Hironori Kiyooka:** Visualization. **Shota Takemura:** Data curation, Proofread. **Kazuyoshi Ogasawara:** Supervision, Software, Validation.

Declaration of competing interest

The authors declare that they have no known competing financial interests or personal relationships that could have appeared to influence the work reported in this paper.

Acknowledgement

We acknowledge the support from Siti Nurfadilah and Retno Setianingsih, students of Magister Pendidikan IPA, Universitas PGRI Semarang.

References

[1] P. Hohenberg, W. Kohn, Inhomogeneous electron gas, Phys. Rev. 136 (3B) (1964) B864.
[2] W. Kohn, L.J. Sham, Self-consistent equations including exchange and correlation effects, Physical review 140 (4A) (1965) A1133.
[3] H. Adachi, M. Tsukada, C. Satoko, Discrete variational Xα cluster calculations. I. Application to metal clusters, J. Phys. Soc. Japan 45 (3) (1978) 875–883.
[4] T. Tanabe, H. Adachi, S. Imoto, Hartree-Fock-slater model cluster calculations. II. Hydrogen chemisorption on transition metal surfaces, Jpn. J. Appl. Phys. 17 (1) (1978) 49.
[5] H. Adachi, S. Shiokawa, M. Tsukada, C. Satoko, S. Sugano, Discrete variational xα cluster calculations. III. Application to transition metal complexes, J. Phys. Soc. Japan 47 (5) (1979) 1528–1537.
[6] J.L. Martins, N. Troullier, S.H. Wei, Pseudopotential plane-wave calculations for ZnS, Phys. Rev. B 43 (3) (1991) 2213.
[7] N. Troullier, J.L. Martins, Efficient pseudopotentials for plane-wave calculations, Phys. Rev. B 43 (3) (1991).
[8] P. Blaha, K. Schwarz, P. Sorantin, S.B. Trickey, Full-potential, linearized augmented plane wave programs for crystalline systems, Comput. Phys. Commun. 59 (2) (1990) 399–415.
[9] W.Y. Ching, Theoretical studies of the electronic properties of ceramic materials, J. Am. Ceram. Soc. 73 (11) (1990) 3135–3160.
[10] J.C. Parker, D.J. Lam, Y.N. Xu, W.Y. Ching, Optical properties of vanadium pentoxide determined from ellipsometry and band-structure calculations, Phys. Rev. B 42 (8) (1990) 5289.
[11] B. Walker, First-principles calculation of laser crystal multiplet levels via hybridized density functional theory and configuration interaction within the OLCAO method, Adv. Sustain. Sci. Eng. Technol. 1 (1) (2019), 0190101.
[12] K. Ogasawara, T. Ishii, Y. Ito, H. Ida, I. Tanaka, H. Adachi, Analysis of covalent effects on the multiplet structure of ruby based on first-principles cluster calculations, Jpn. J. Appl. Phys. 37 (8) (1998) 4590–4594.
[13] K. Ogasawara, T. Ishii, I. Tanaka, H. Adachi, Calculation of multiplet structure of ruby using explicit effective Hamiltonian, Mater. Trans., JIM 40 (No. 5) (1999) 396–399.
[14] K. Ogasawara, T. Ishii, I. Tanaka, H. Adachi, Calculation of multiplet structures of Cr^{3+} and V^{3+} in α-Al2O3 based on a hybrid method of density-functional theory and the configuration interaction, Phys. Rev. B 61 (1) (2000) 143–161.
[15] K. Ogasawara, T. Iwata, Y. Koyama, T. Ishii, I. Tanaka, H. Adachi, Relativistic cluster calculation of ligand-field multiplet effects on cation $L_{2,3}$ x-ray-absorption edges of $SrTiO_3$, NiO, and CaF_2, Phys. Rev. B 64 (11) (2001) 115413.
[16] K. Ogasawara, T. Miyamae, I. Tanaka, H. Adachi, First-principles calculation of transition-metal $L_{2,3}$-edge electron-energy-loss near-edge structures based on direct diagonalization of the many-electron Hamiltonian, Mater. Trans. 43 (7) (2002) 1435–1438.
[17] K. Ogasawara, S. Watanabe, Y. Sakai, H. Toyoshima, T. Ishii, M.G. Brik, I. Tanaka, Calculations of complete 4 f n and 4 f n -1 5 d 1 energy level schemes of free trivalent rare-earth ions, Jpn. J. Appl. Phys. 43 (5A) (2004). L611–L613.
[18] K. Ogasawara, S. Watanabe, T. Ishii, M.G. Brik, Relativistic calculations of complete $4f^n$ energy level schemes of free trivalent rare-earth ions, Jpn. J. Appl. Phys. 44 (10) (2005) 7488–7490.
[19] M. Novita, K. Ogasawara, Comparative study of absorption spectra of V^{2+}, Cr^{3+}, and Mn^{4+} in α-Al_2O_3 based on first-principles configuration-interaction calculations, J. Phys. Soc. Jpn. 81 (10) (2012) 104709.
[20] M. Novita, D. Marlina, N. Cholifah, K. Ogasawara, Study on the molecular orbital energies of ruby under pressure, Opt. Mater. (Amst). 109 (1) (2020) 110375.
[21] M. Novita, D. Marlina, N. Cholifah, K. Ogasawara, Enhance electron-correlation effect on the ruby multiplet energy dependence on pressure, Opt. Mater. (Amst). 110 (2020) 110520.
[22] M. Novita, K. Ogasawara, Comparative study of multiplet structures of Mn^{4+} in K_2SiF_6, K_2GeF_6, and K_2TiF_6 based on first-principles configuration–interaction calculations, Jpn. J. Appl. Phys. 51 (2R) (2012) 022604.
[23] M. Novita, K. Ogasawara, Study on multiplet energies of V^{2+}, Cr^{3+}, and Mn^{4+} in MgO host crystal based on first-principles calculations with consideration of lattice relaxation, J. Phys. Soc. Jpn. 83 (12) (2014) 124707.
[24] M. Novita, T. Honma, B. Hong, A. Ohishi, K. Ogasawara, Study of multiplet structures of Mn^{4+} activated in fluoride crystals, J. Lumin. 169 (2016) 594–600.
[25] M. Novita, H. Yoshida, K. Ogasawara, Investigation of ion dependence of electronic structure for $3d^3$ ions in Mg_2TiO_4 based on first-principles calculations, ECS Transactions 50 (41) (2012) 9–17.
[26] M. Novita, D. Marlina, K. Ogasawara, K.J. Seok, K.Y. Soo, Study on the optical luminescence properties of Li_2TiO_3: Mn^{4+} and Cr^{3+}, Chem. Lett. 50 (1) (2021) 52–56.
[27] S. Watanabe, K. Ogasawara, Experimental and first-principles analysis of 4f-5d absorption spectrum for Ce^{3+} in $LiYF_4$ considering lattice relaxation, J. Phys. Soc. Jpn. 77 (8) (2008) 1–7.
[28] W.D. Wright, A trichromatic colorimeter with spectral primaries, Trans. Opt. Soc. 29 (5) (1928) 225.
[29] W.D. Wright, A re-determination of the trichromatic coefficients of the spectral colours, Trans. Opt. Soc. 30 (4) (1929) 141.
[30] R.W.G. Hunt, M.R. Pointer, A colour-appearance transform for the CIE 1931 standard colorimetric observer, Color Res. Appl. 10 (3) (1985) 165–179.
[31] A.D. Broadbent, A critical review of the development of the CIE1931 RGB color-matching functions, Color Res. Appl. 29 (4) (2004) 267–272.
[32] H.S. Fairman, M.H. Brill, H. Hemmendinger, How the CIE 1931 color-matching functions were derived from Wright-Guild data, Color Res. Appl. 22 (1) (1997) 11–23.
[33] H. Sawada, Residual electron density study of α-aluminum oxide through refinement of experimental atomic scattering factors, Mater. Res. Bull. 29 (2) (1994) 127–133.
[34] R.D. Cowan, The Theory of Atomic Structure and Spectra, University of California Press, Berkeley, CA, 1981, p. 461, 1981.
[35] W.M. Fairbank, G.K. Klauminzer, A.L. Schawlow, Excited-state absorption in ruby, emerald, and MgO: Cr^{3+}, Phys. Rev. B 11 (1) (1975) 60–76.
[36] P. Kizler, Structural relaxation around Substitutional Cr^{3+} ions in Saphire, J. Am. Ceram. Soc. 79 (1996) 3–11.

2021_OptMat_Mega_Novita_CIE_Ruby.pdf

ORIGINALITY REPORT

24%	20%	16%	5%
SIMILARITY INDEX	INTERNET SOURCES	PUBLICATIONS	STUDENT PAPERS

PRIMARY SOURCES

1	www.avantes.com Internet Source	3%
2	hdl.handle.net Internet Source	3%
3	journals.jps.jp Internet Source	2%
4	"Hartree-Fock-Slater Method for Materials Science", Springer Nature, 2006 Publication	2%
5	Mega Novita, Kazuyoshi Ogasawara. " Comparative Study of Absorption Spectra of V , Cr , and Mn in α-Al O Based on First-Principles Configuration–Interaction Calculations ", Journal of the Physical Society of Japan, 2012 Publication	2%
6	icomonline.org Internet Source	1%
7	bak.spm.com.cn Internet Source	1%

8	epdf.pub Internet Source	1 %
9	K. Ogasawara, S. Watanabe, H. Toyoshima, T. Ishii, M.G. Brik, H. Ikeno, I. Tanaka. "Optical spectra of trivalent lanthanides in LiYF4 crystal", Journal of Solid State Chemistry, 2005 Publication	1 %
10	M.G. Brik, K. Ogasawara. "First-principles calculations of the V3+ absorption spectra in LiAlO2 and LiGaO2", Journal of Non-Crystalline Solids, 2006 Publication	1 %
11	ebin.pub Internet Source	<1 %
12	qlkh.humg.edu.vn Internet Source	<1 %
13	link.springer.com Internet Source	<1 %
14	mospace.umsystem.edu Internet Source	<1 %
15	Philippe Gérard. "Color Segmentation and Color Correction Using Lighting and White Balance Shifts", Lecture Notes in Computer Science, 1998 Publication	<1 %
16	rcin.org.pl	

Internet Source <1%

17 telescript.denayer.wenk.be
Internet Source <1%

18 K. Damak, E. Yousef, S. AlFaify, C. Rüssel, R. Maâlej. "Raman, green and infrared emission cross-sectionsof Er^3+ doped TZPPN tellurite glass", Optical Materials Express, 2014
Publication <1%

19 Novita, Mega, and Kazuyoshi Ogasawara. "Comparative Study of Multiplet Structures of Mn4+ in K2SiF6, K2GeF6, and K2TiF6 Based on First-Principles Configuration–Interaction Calculations", Japanese Journal of Applied Physics, 2012.
Publication <1%

20 www.duo.uio.no
Internet Source <1%

21 Ishii, Takugo, K. Fujimura, K. Ogasawara, I. Tanaka, and H. Adachi. "", Laser Optics 2000 Solid State Lasers, 2001.
Publication <1%

22 Derek W. Smith. "Ligand Field Theory & Spectra", Encyclopedia of Inorganic Chemistry, 03/15/2006
Publication <1%

aip.scitation.org

23	Internet Source	<1%
24	Satoshi Motozuka, Motohiro Tagaya, Toshsiyuki Ikoma, Masahiko Morinaga, Tomohiko Yoshioka, Junzo Tanaka. "Efficient Methane Conversion to Hydrogen by the Force-Activated Oxides on Iron Particle Surfaces", The Journal of Physical Chemistry C, 2013 Publication	<1%
25	Takugo Ishii. "Theoretical calculation for the multiplet structure of the tetrahedrally coordinated Cr[sup 4+] in Y[sub 3]Al[sub 5]O[sub 12]", The Journal of Chemical Physics, 2001 Publication	<1%
26	repository.wima.ac.id Internet Source	<1%
27	Dorneich, French, Müllejans, Loughin, Rühle. "Quantitative analysis of valence electron energy - loss spectra of aluminium nitride", Journal of Microscopy, 2001 Publication	<1%
28	Mega Novita, Nur Cholifah, Kazuyoshi Ogasawara. "Lattice Relaxation Effects on the Multiplet Energies of Ruby Under Pressure using One-Electron Calculations", IOP	<1%

	Conference Series: Materials Science and Engineering, 2020 Publication	
29	academic.oup.com Internet Source	<1 %
30	docksci.com Internet Source	<1 %
31	en.wikipedia.org Internet Source	<1 %
32	etd.adm.unipi.it Internet Source	<1 %
33	www.ingenieria.cl Internet Source	<1 %
34	www.science.gov Internet Source	<1 %
35	Joanne Zwinkels. "Surface Fluorescence: the Only Standardized Method of Measuring Luminescence", Springer Series on Fluorescence, 2008 Publication	<1 %
36	Teruyasu Mizoguchi, Weine Olovsson, Hidekazu Ikeno, Isao Tanaka. "Theoretical ELNES using one-particle and multi-particle calculations", Micron, 2010 Publication	<1 %

37	The DV-Xα Molecular-Orbital Calculation Method, 2015. Publication	<1%
38	Kazuyoshi Ogasawara, Shinta Watanabe. "Current Situation and Future Development of Discrete Variational Multielectron Method", Elsevier BV, 2008 Publication	<1%
39	M. G. Brik. "Comparative first-principles analysis of the absorption spectra of ZnAl2S4 and ZnGa2O4 crystals doped with Cr3+", The European Physical Journal B, 2006 Publication	<1%

Exclude quotes	On	Exclude matches	Off
Exclude bibliography	On		